MCB
Journals.ASM.org

Luman/CREB3 Recruitment Factor Regulates Glucocorticoid Receptor Activity and Is Essential for Prolactin-Mediated Maternal Instinct

Amanda C. Martyn,[a]* Elena Choleris,[b] Daniel J. Gillis,[c] John N. Armstrong,[a,d] Talya R. Amor,[a] Adam R. R. McCluggage,[a] Patricia V. Turner,[e] Genqing Liang,[a]* Kimberly Cai,[a] and Ray Lu[a]

Departments of Molecular and Cellular Biology,[a] Psychology,[b] Mathematics and Statistics,[c] Biomedical Sciences,[d] and Pathobiology,[e] University of Guelph, Guelph, Ontario, Canada

The hypothalamic-pituitary-adrenal (HPA) axis is a major part of the neuroendocrine system in animal responses to stress. It is known that the HPA axis is attenuated at parturition to prevent detrimental effects of glucocorticoid secretion including inhibition of lactation and maternal responsiveness. Luman/CREB3 recruitment factor (LRF) was identified as a negative regulator of CREB3 which is involved in the endoplasmic reticulum stress response. Here, we report a LRF gene knockout mouse line that has a severe maternal behavioral defect. *LRF*$^{-/-}$ females lacked the instinct to tend pups; 80% of their litters died within 24 h, while most pups survived if cross-fostered. Prolactin levels were significantly repressed in lactating *LRF*$^{-/-}$ dams, with glucocorticoid receptor (GR) signaling markedly augmented. In cell culture, LRF repressed transcriptional activity of GR and promoted its protein degradation. LRF was found to colocalize with the known GR repressor, RIP140/NRIP1, which inhibits the activity by GR within specific nuclear punctates that are similar to LRF nuclear bodies. Furthermore, administration of prolactin or the GR antagonist RU486 restored maternal responses in mutant females. We thus postulate that LRF plays a critical role in the attenuation of the HPA axis through repression of glucocorticoid stress signaling during parturition and the postpartum period.

The maternal response in mice is a set of well-characterized, fundamental behaviors that include nest building, pup retrieval, and crouching over pups (52). Hormonal control is critical for development of the maternal response (4, 5, 31). Prolactin (PRL), in particular, a polypeptide hormone synthesized in the anterior pituitary, is implicated in rapid stimulation of maternal behavior (5, 39) in addition to its role in induction of lactation (36). Activation of PRL synthesis is under the control of a single protein, pituitary-specific transcription factor 1 (Pit-1) (17, 40). Key regulators of PRL synthesis and secretion are glucocorticoids, which inhibit PRL through glucocorticoid receptor (GR) binding to the PRL promoter (3). GR may also repress PRL synthesis through interference with PRL transcription activation by Pit-1 (47).

Glucocorticoid secretion is triggered by the hypothalamic-pituitary-adrenal (HPA) axis in response to both physical and psychological stresses. Stress signals rapidly stimulate corticotrophin-releasing hormone (CRH) and vasopressin neurons in the hypothalamic paraventricular nucleus (PVN), which subsequently induce adrenocorticotrophic hormone (ACTH) secretion in the anterior pituitary, leading to adrenal cortex glucocorticoid secretion. Sustained high levels of glucocorticoids are detrimental, and rapid glucocorticoid negative feedback is critical in the termination of HPA axis activation (10). It is known that prolonged activation of the HPA axis and glucocorticoid signaling contribute to poor parental care (24, 30, 49). The HPA axis is closely modulated in mammals during pregnancy and at parturition (37); however, the mechanism underlying GR regulation and attenuation of the HPA axis is unclear (2, 44).

Recent reports implicate the endoplasmic reticulum (ER) stress-related Luman or cyclic AMP response element binding protein 3 (Luman/CREB3) (38) in the regulation of GR (34). The negative regulator Luman/CREB3 recruitment factor (LRF) targets Luman/CREB3 to discrete nuclear foci and represses its activity (1). To study the biological role of LRF, we created a gene knockout mouse line. *LRF*$^{-/-}$ mice have a severe deficit in maternal behavior accompanied by low levels of circulating PRL. We also found that LRF represses GR, which may lead to PRL misregulation through altered HPA axis sensitivity to glucocorticoids in these mice.

MATERIALS AND METHODS

Animals. This study followed the Canadian Council of Animal Care guidelines and was approved by the Animal Care Committee at the University of Guelph. The *LRF* gene knockout mouse line was generated in collaboration with the International Gene Trap Consortium (48). Chimeric mice were backcrossed to C57BL/6 mice (Charles River, Montreal, Canada) to produce a >99.9% congenic mouse strain. Mice were group housed with same-sex siblings (from weaning to 24 h prior to test date) and maintained on a 12-h reversed light/dark cycle (1000 to 2200 h). Temperature was maintained at 21 to 24°C; food (14% standard diet; Harland Teklad) and water were provided *ad libitum*. PRL-treated dams were injected subcutaneously (s.c.) twice daily with 5 mg/ml PRL from sheep pituitary (Sigma) in 0.9% sodium chloride or vehicle alone, commencing at 18 days postcoitum (dpc).

Behavior testing. Animals derived from *LRF*$^{+/-}$ crosses, 3 to 5 months of age, were housed individually 24 h prior to testing. Tests were performed during the active period (1100 to 1700 h). On the day of test-

Received 20 August 2012 Returned for modification 30 September 2012
Accepted 8 October 2012
Published ahead of print 15 October 2012
Address correspondence to Ray Lu, rlu@uoguelph.ca.
* Present address: Amanda C. Martyn, Department of Medicine: Gastroenterology, Duke University, Durham, North Carolina, USA; Genqing Liang, Laboratory of Molecular Immunogenetics, National Institute of Arthritis and Musculoskeletal and Skin Diseases, NIH, Bethesda, Maryland, USA.
Supplemental material for this article may be found at http://mcb.asm.org/.
Copyright © 2012, American Society for Microbiology. All Rights Reserved.
doi:10.1128/MCB.01142-12

ing, mice were moved to a testing room and allowed to habituate for 1 h. All tests were performed under red light, counterbalanced for placement where applicable, with the exception of the dark-light test, which was performed in a brightly lit room, and tests were videotaped for subsequent analysis with Observer Video Analysis (Noldus, Wageningen, The Netherlands). Data were scored blindly by a single, impartial, third party. All testing apparatus was cleaned between each mouse with Alconox detergent (Prolab Scientific, Laval, Quebec, Canada) in water, followed by an aqueous baking soda solution.

(i) Dark-light test. Each mouse was placed in a clear polycarbonate square box divided by a black insert into dark and light rectangular compartments of equal sizes (16 in. long by 8 in. wide by 5 in. high) with an entry opening of 4 in. long by 1.25 in. high (AccuScan Instruments, Columbus, OH). Mice were released in a corner of the dark area, and their activity was tracked by a set of three photo beam arrays for 5 min. The test was repeated 24 h later. All data were collected using a VersaMax Analyser (AccuScan Instruments).

(ii) Social recognition test. The social recognition paradigm was modified from previous studies (12, 13). Briefly, each test mouse was individually placed in a testing cage (23 by 23 by 33 cm) containing two Plexiglas perforated cylinders (7-cm diameter; 12 cm high) in the corners of the long side of the cage. Ovariectomized CD1 mice, 3 to 4 months of age, were used as stimuli. Each test mouse was exposed four times (T1 to T4) to two stimulus mice, one in each cylinder, for 5 min. Intertest intervals (ITIs; when stimulus mice were removed) lasted 15 min. On a fifth exposure (T5), a novel stimulus mouse was introduced, paired with a familiar stimulus mouse. Active sniffing in the holes of the cylinder was used as a measure of social investigation, as previously reported (12).

(iii) Hidden-reward olfaction test. All mice were food deprived for 17 to 20 h prior to testing. Each mouse was allowed to consume 1/12 of a Hershey's chocolate chip, placed on the surface of the bedding. Five minutes later, 1/4 of a chocolate chip was buried in the bedding away from the mouse, and the time it took the mouse to find the chocolate chip was measured.

(iv) Pup retrieval assay. Adult wild-type (WT) and $LRF^{-/-}$ virgin female mice were housed individually and provided with cotton bedding 24 h prior to pup exposure. Test mice were exposed to three 1- to 3-day-old WT pups for 10 min per day on three consecutive days. Pups were introduced into a corner of the cage not containing the nest. Pup-related (crouching and licking) and non-pup-related (nest building and locomotor activity) behaviors were collected on the third day of exposure, and at the end of each test, the quality of the nest was scored from 0 (no nest) to 3 (complete nest) as previously described (32). For RU486 treatment, mice were injected with 7.5 mg/kg RU486 (mifepristone; Sigma) in water (or vehicle alone) 1 h prior to each test and tested for 4 days.

Statistical analysis of behavior. In all tests, data were analyzed using a significance level of 0.05 (*P* value).

(i) Tail suspension and litter survival. A *Z* test for proportions, comparing between genotypes (or treatment within genotype for the PRL exposure experiment), was used. Refer to supporting information in the supplemental material.

(ii) Hidden-reward olfaction, RU486, and pup retrieval tests. A two-tailed *t* test, comparing between genotypes within each group (male and female) was used.

(iii) Dark-light and social recognition tests. General linear models were conducted using SAS, version 9.1 (SAS Institute Inc.), and the *R* statistical software package (www.R-project.org). All alternative hypotheses were tested against a null. For detailed analysis on each test, refer to supporting information in the supplemental material.

RNA analysis. Total RNA was isolated with TRIzol (Invitrogen, Carlsbad, CA) from adult mouse tissues. Synthesis of cDNA was performed using SuperScript III reverse transcriptase (Invitrogen) and oligo(dT) (Roche Diagnostics, Laval, QC, Canada). Reverse transcriptase PCR (RT-PCR) amplification of mouse *LRF* mRNA was performed using primers P4 (5′-CTGCCAGCACTTCTGTTTCA) and P5 (5′-AAGCTCTGGATG CCAGCTTA) (Fig. 1); human *LRF* mRNA from HeLa cells was amplified using primers 5′-GCCTCTTCAAGGTCATGCCA and 5′-AAGTGACCC AGGACCTTCCTG; and β-actin mRNA was amplified using primers 5′-GAGAAGATCTGGCACCACACC and 5′-CAAGAAGGAAGGCTGGAA AAG.

Northern blotting. RNA probes were prepared following the manufacturer's instructions using a digoxigenin (DIG) RNA labeling kit (Roche). A 575-bp cDNA insert encoding exons 2 to 4 of mouse *LRF* (primers P6, 5′-ACTCACAGGATCTGGGCTTG, and P7 5′-GGCAGCT GCTCTATTTGTGG) (Fig. 1) in the pCRII-TOPO vector (Invitrogen) was used to generate an antisense RNA probe. Total RNA (10 μg) was subjected to electrophoresis on a 1.2% agarose gel and hybridized with 100 ng/ml of DIG-labeled RNA probes.

Whole-brain sectioning. Animals were overdosed (120 mg/kg) with sodium pentobarbital (Ceva Santé Animale, Libourne, France) and perfused through the ascending aorta with phosphate-buffered saline (1× PBS) followed by 2% paraformaldehyde (PFA) in 1× PBS, pH 6.5. Whole brains were extracted, postfixed for 2 h at room temperature, and sectioned at 50 μM on a Leica VT1000S vibrating microtome (Leica Microsystems Canada, Inc., Richmond Hill, ON, Canada).

X-Gal staining. Floating sections were fixed for 2 h in 4% PFA in 1× PBS, pH 6.5, rinsed in buffer (100 mM sodium phosphate, pH 7.3, 2 mM $MgCl_2$, 0.1% Triton X-100), prestained for 1 h in rinse buffer containing 5 mM potassium ferrocyanide–5 mM potassium ferricyanide, and stained for >12 h at 37°C in prestain solution containing 4 mg/ml 5-bromo-4-chloro-3-indolyl-β-D-galactopyranoside (X-Gal). Sections were postfixed for 18 h in 4% PFA containing 0.25% glutaraldehyde. Images were captured with a Micropublisher 5.0 digital camera (QImaging, Surrey, BC, Canada) and QCapture software (QImaging) under a Leica MZ125 dissecting microscope (Leica).

Histological assessment of mouse tissue. Mammary tissues were fixed in 4% PFA in 1× PBS (pH 8.5) and sectioned at 10 μM thickness. All mammary tissues were blind coded and scored by a clinical pathologist. Images were captured on a Leica DMRA2 microscope with a Hamamatsu ORCA-ER digital camera and Openlab imaging software (PerkinElmer, Waltham, MA).

Immunohistochemistry. Floating sections were rinsed in 1× Tris-buffered saline (TBS), pH 7.0, plus 0.6% sodium azide, followed by three washes in 1× TBS, pH 7.0, and blocked for 1 h at room temperature in 1× TBS containing 0.1% Triton X-100, 3% goat serum, and 0.05% (wt/vol) bovine serum albumin (BSA) before incubation for 18 h at 4°C with the following primary antibodies: MAP2 (Abcam Inc., Cambridge, MA) at 1/3,000 and β-galactosidase (β-Gal; US Biological, Houston, TX) at 1/1,000. Sections were rinsed three times in 1× TBS and incubated for 1 h in 1× TBS containing the following secondary antibodies: Alexa 488-conjugated antibody (Invitrogen) for β-Gal at 1/4,000 and Alexa 594-conjugated antibody (Invitrogen) for MAP2 at 1/10,000. Images were captured with an Axiocam Mrc5 camera (Carl Zeiss Canada Ltd., Toronto, Ontario, Canada) under an Axio Imager D1 (Carl Zeiss Canada Ltd.) with Axio Vision, version 4.6, software (Carl Zeiss Canada Ltd.).

ELISAs. Blood samples (100 to 150 μl) were collected in the active cycle (1000 to 1100 h) from the saphenous vein of the hind limb; serum was collected and stored at −80°C. Hormone levels were detected using a mouse/rat PRL enzyme-linked immunosorbent assay (ELISA) kit (Calbiotech, Spring Valley, CA), a corticosterone enzyme immunoassay (EIA) kit (Assay Designs, Ann Arbor, MI), or an oxytocin EIA kit (Assay Designs, Ann Arbor, MI), as per the manufacturers' instructions, and detected using a POLARstar Omega plate reader (BMG Labtech GmbH, Offenburg, Germany). Statistical analysis was performed using two-way repeated measures analysis of variance (ANOVA) and a pairwise multiple comparison procedure where applicable. Data were deemed significant at a *P* value of <0.05.

Plasmids. The pEGFP-LRF (where EGFP is enhanced green fluorescent protein) and pFLAG-LRF plasmids were constructed previously (1). The pRL-SV40 plasmid (Promega) contains the *Renilla reniformis* lucif-

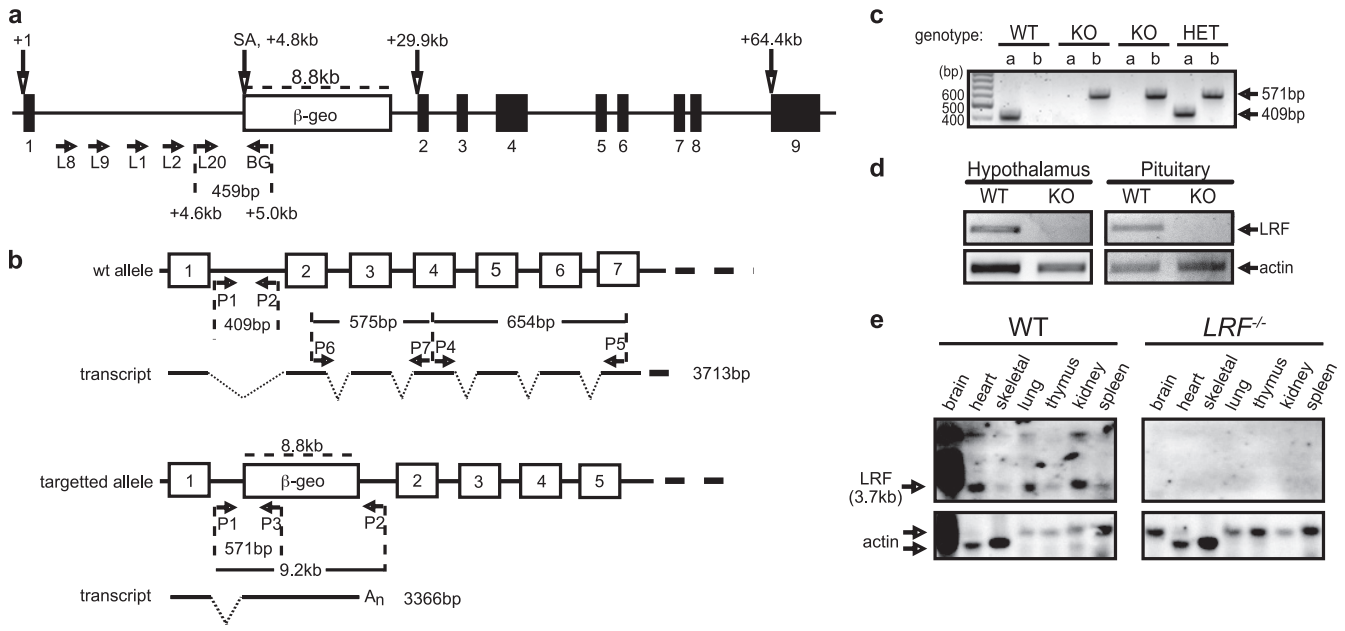

FIG 1 Genotypic confirmation of the *LRF* KO mice. (a) Mapping the *LRF*-β-*geo* locus. A series of primers were designed within intron 1 of the *LRF* allele (L8, L9, L1, L2, and L20) in pair with a primer (BG) situated 200 bp inside the β-*geo* cassette, downstream of the splice acceptor (SA) sequence. The L20/BG combination of primers revealed a 459-bp sequence by PCR that was sequenced to confirm identity and positioning of the β-*geo* cassette which is 4.8 kb downstream of the transcription start site. (b) Genotyping strategy showing expected transcripts from the WT and disrupted alleles, with only five or seven of the total nine exons shown. A_n stands for poly(A) tail. (c) A typical genotyping result by PCR, using primers P1 and P2 (WT allele) or P1 and P3 (knockout [KO] allele) on tail snip DNA. The 409-bp band identifies a wild-type (WT) allele, and a 571-bp band indicates the targeted null (KO) allele. HET, $LRF^{+/-}$. (d) *LRF* detection by RT-PCR in WT and $LRF^{-/-}$ mature female mouse tissues using primers P4 and P5, downstream of the β-geo cassette insertion site. A 656-bp RT-PCR fragment of *LRF* exons 4 to 7 was detected in the WT but not in the $LRF^{-/-}$ tissues. β-*actin* was used as a loading control. (e) Confirmation of the *LRF* KO genotype by Northern blotting using DIG-labeled RNA probes spanning exons 2 to 4 (P6 and P7). A distinct 3.7-kb band was identified in WT but absent in $LRF^{-/-}$ mouse tissues. LRF transcripts are highly abundant in the WT mouse brain, with larger transcripts likely representing incompletely spliced mRNA. Heart and skeletal actin has two forms, running at approximately 2.1 kb and 1.8 kb (17a).

erase gene under the control of the simian virus 40 (SV40) immediate-early promoter. The pEGFP-RIP140 (where RIP140 is receptor-interacting protein 140), pSG5-hGR, and pMMTV-Luc (containing the firefly luciferase gene; MMTV is mouse mammary tumor virus) were provided by Johanna Zilliacus, Karolinska Institutet (63), Jorma Pavlimo, University of Helsinki (45), and Ronald Evans, Howard Hughes Medical Institute, respectively (22).

Cell culture. HeLa cells were grown in monolayer culture in Dulbecco's modified Eagle's medium (high glucose) supplemented with 10% (vol/vol) fetal bovine serum (Invitrogen), 100 IU/ml penicillin, and 100 μg/ml streptomycin. All cultures were maintained in a 5% CO_2 humidified atmosphere at 37°C and passaged every 2 to 3 days. Cells were plated 24 h prior to transfection and allowed to grow to 60% confluence prior to transfection. Cells were transfected by FuGENE HD transfection reagent (Roche) as per the manufacturer's instruction.

Dual-luciferase assays. HeLa cells were plated in six-well plates and cotransfected with 0.5 μg of pMMTV-Luc, 80 ng of pRL-SV40, and 0.25 μg of pSG5-hGR, together with 1 μg of pEGFP-LRF (or pcDNA3.1) and 0.5 μg of pEGFP-RIP140 (or pcDNA3.1). At 24 h posttransfection, the medium was changed, and 100 nM dexamethasone (Dex) was added as required for 8 h. Cells were lysed, and dual-luciferase assays were performed according to the manufacturer's instructions (Promega Corporation, Madison, WI). Relative luciferase activity was calculated (firefly luciferase/*Renilla* luciferase) to correct for transfection efficiency. Assays were independently repeated three times, and data are represented with standard errors of the means (SEM).

Immunofluorescence confocal microscopy. HeLa cells were plated on glass coverslips in six-well plates and transfected (or cotransfected) with 1 μg of pSG5-hGR, pEGFP-LRF, pEGFP-RIP140, and FLAG-LRF in the combinations indicated in Fig. 6. Cells were treated for 8 h with 100 nM Dex and 5 μM MG132 (EMD Biosciences, San Diego, CA) to prevent protein degradation by the proteosome prior to fixation. Primary antibodies were used at the following dilutions: GR polyclonal antibody (H-300; Santa Cruz Biotechnology, Inc., Santa Cruz, CA) at 1/500 and FLAG monoclonal antibody (M2; Sigma) at 1/500. Secondary Alexa 488- and Alexa 594-conjugated antibodies were used at 1/1,000 (Invitrogen). Transfected cells were incubated in antibodies for 35 min and mounted in 50% glycerol with 0.5 nM 4′,6′-diamidino-2-phenylindole (DAPI). Images were captured with a Hamamatsu ORCA-ER digital camera under a Leica DMRE confocal microscope.

CHX assay. HeLa cells were plated in 12-well plates and transfected at 60% confluence with 1 μg of pSG5-hGR alone or cotransfected with 1 μg of pSG5-hGR and 1 μg of pEGFP-LRF. At 24 h posttransfection, cells were treated with 100 nM Dex and at 0, 2, 4, and 6 h with 50 μg/ml cycloheximide (CHX; Sigma). Cells were harvested and used for subsequent analysis.

Western blotting. Primary antibodies were used at the following dilutions: GR polyclonal antibody (H-300; Santa Cruz) at 1/1,000, FLAG monoclonal antibody (M2; Sigma) at 1/1,000, GFP polyclonal antibody (Roche) at 1/1,000, and β-actin monoclonal antibody (clone AC-15; Sigma) at 1/1,000. Secondary horseradish peroxidase (HRP)-conjugated antibodies were used at 1/20,000 (Promega). Blots were visualized using ECL Plus (GE Healthcare, Piscataway, NJ) on Amersham Hyperfilm ECL (GE Healthcare).

qRT-PCR. Transcript levels were measured by quantitative RT-PCR (qRT-PCR) using PerfeCTa SYBR green Supermix with 6-carboxy-X-rhodamine (ROX) (Quanta Biosciences, Inc., Gaithersburg, MD) and primers against the mouse genes, PRL (5′-ATGTTCAGCCTCTGCC AATC and 5′-GAAGTGGGGCAGTCATTGAT), PRLR (5′-CCTGCATC TTTCCACCAGTT and 5′-CCAGCAAGTCCTCACAGTCA), Csn2 (5′-G

ACAGCTGCAGGCAGAGGAT and 5′-GACGGGATTGCAAGAGAT GG), interferon regulatory factor (IRF-1) (5′-AACCAAATCCCAGGGC TGAT and 5′-CTCCGGAACAGACAGGCATC), insulin-like growth factor binding protein 1 (IGFBP1) (5′-GAGGATCAGCCCATCCTGTG and 5′-GCAGGGCTCCTTCCATTTCT), and actin (5′-CCTGAACCCT AAGGCCAACC and 5′-CACAGCCTGGATGGCTACG). Samples were run on a StepOnePlus Real-Time PCR System (Applied Biosystems, Carlsbad, CA) and subjected to standard curve analysis, and arbitrary values were represented, adjusting for primer efficiencies. To ensure that appropriate primer-specific products were produced, melting curve analyses were performed on the SYBR green channel using a ramping rate of 1°C/30 s from 60 to 95°C. Data are presented as the averages of three technical repeats from two independent sample sets that consisted of pooled RNA from three animals and are standardized to β-actin values.

RESULTS

Generation of LRF$^{-/-}$ mice. Our gene knockout mice represent a gene-trapped line that contains a β-galactosidase (β-Gal)/neomycin phosphotransferase II fusion gene (β-*geo*) (48) inserted into intron 1 of the *LRF* gene. The disrupted allele in the F1 progeny of chimeric mice was confirmed by PCR and DNA sequencing (Fig. 1a). Heterozygous (*LRF*$^{+/-}$) mice were backcrossed to C57BL/6 mice for >11 generations to produce a >99.9% congenic C57BL/6 strain before data collection.

Genotyping LRF mice was performed using primers designed against LRF genomic DNA (Fig. 1b, P1 and P2) and the targeted allele (Fig. 1b, P1 and P3). The presence of a 409-bp band identifies a wild-type (WT) allele, and a 571-bp band indicates the targeted null allele (Fig. 1c).

Confirmation of the functional *LRF* knockout was accomplished by RT-PCR (Fig. 1d) and Northern blot analysis (Fig. 1e) on adult mouse tissues. To rule out the possibility of downstream methionine start sites that could produce shorter LRF isoforms, two different regions downstream of the cassette insertion were targeted. A 656-bp RT-PCR fragment of LRF exons 4 to 7 (Fig. 1b, P4 and P5) was detected in the wild-type but not in the null (LRF$^{-/-}$) tissues of male (not shown) and female mice (Fig. 1d). Further, using an RNA probe spanning exons 2 to 4 (Fig. 1b, between P6 and P7), a distinct 3.7-kb band was identified in WT tissues but was absent in LRF$^{-/-}$ mouse tissues, demonstrating that no WT LRF mRNA was transcribed (Fig. 1e). It is of interest that LRF transcripts are highly abundant in the WT mouse brain, with larger transcripts likely representing incompletely spliced mRNA variants (Fig. 1e). The high abundance of LRF was also confirmed by X-Gal staining (see Fig. S1 in the supplemental material) since β-*gal* gene expression in the mutant LRF allele is under the control of the LRF promoter (Fig. 1b), which gave a neuron-specific staining pattern.

Gross and microscopic assessment of the mutant mouse tissues found no apparent abnormalities in *LRF*$^{-/-}$ or *LRF*$^{+/-}$ mice compared with the WT although *LRF*$^{-/-}$ mice were significantly smaller in size (see Fig. S2 in the supplemental material). At 6 months of age (170 days), WT male mice weighed 34.7 ± 0.76 g versus 31.96 ± 0.68 g for LRF$^{-/-}$ males (n = 22 and 15, respectively; P = 0.0119). Similarly, adult female WT mice were significantly larger at 27.24 ± 0.75 g than LRF$^{-/-}$ females at 21.99 ± 0.94 g (n = 14 and 8, respectively; P = 0.0005). Intercrosses between *LRF*$^{+/-}$ mice revealed a normal sex ratio and Mendelian genotype distribution (data not shown).

Interestingly, the simple tail suspension test, a nonspecific screen for neurological alterations, revealed that the proportion of mice displaying severe hind limb clasping was significantly higher in *LRF*$^{-/-}$ mice than in WT mice ($P \leq 0.0013$) (see Fig. S3 in the supplemental material). This, along with a neuron-specific expression pattern, implies a neuronal function of LRF.

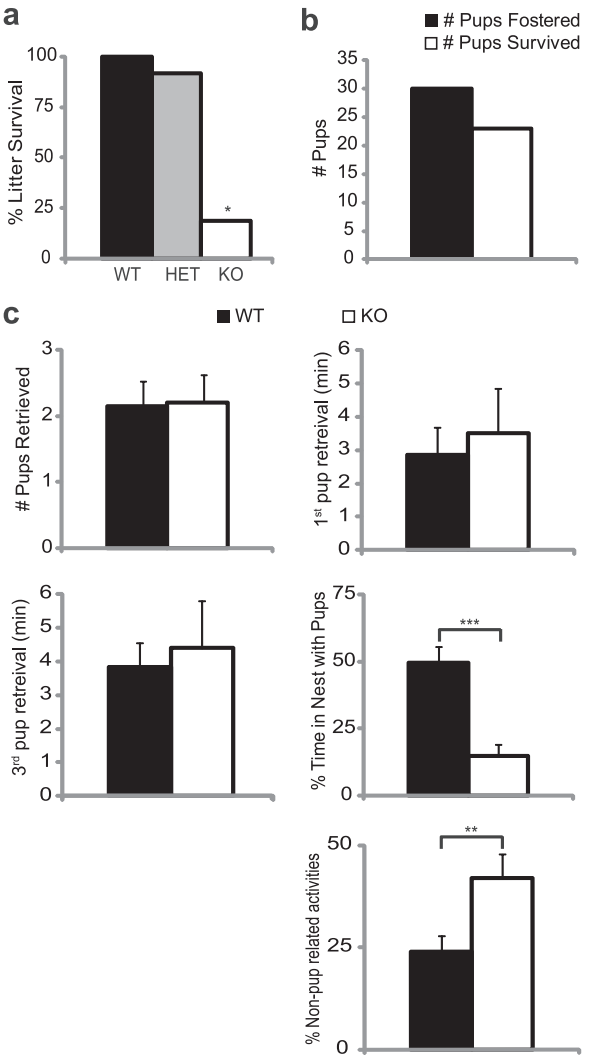

FIG 2 *LRF*$^{-/-}$ female mice display evidence of maternal neglect. (a) Reduced survival of pups born to *LRF*$^{-/-}$ females. The proportion of litters that survived versus litters born was plotted for each maternal genotype. WT (*LRF*$^{+/+}$), n = 26; HET (*LRF*$^{+/-}$), n = 35; KO (*LRF*$^{-/-}$), n = 15. *, $P = 7.65 \times 10^{-10}$ compared to WT in a Z-test for proportions. (b) Cross-fostering pups (n = 30 from 7 litters) from *LRF*$^{-/-}$ to WT dams resulted in a 77% rescue of pup survival (n = 23). (c) Virgin *LRF*$^{-/-}$ females exhibit impaired maternal behavior in a pup retrieval assay. From left to right, top to bottom, adult virgin WT (n = 14) and *LRF*$^{-/-}$ (n = 10) mice were tested for total number of pups retrieved, latency to retrieve the first and third pups, percentage of time spent in the nest with the pups after the first pup was retrieved, and time spent outside the nest, actively engaged in building the nest, digging, or otherwise exploring activities, not including time with pups. **, P = 0.0167; ***, P = 0.0006 (a two-tailed t test).

LRF$^{-/-}$ dams display evidence of maternal neglect. We quickly found that most litters (80%; $P = 7.65 \times 10^{-10}$) produced by *LRF*$^{-/-}$ dams failed to survive beyond 24 h (Fig. 2a); pups were found outside the nest and/or lacking milk spots. In many cases there was evidence of infanticide.

The inbred C57BL/6 mice are generally known to be good

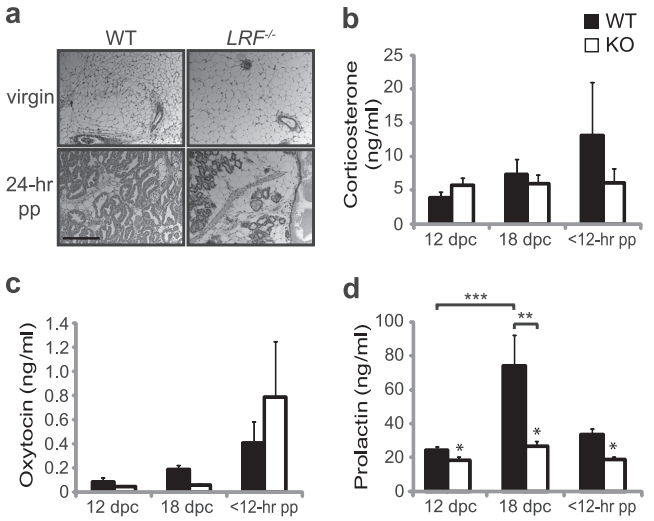

FIG 3 Defect in PRL secretion in $LRF^{-/-}$ mice. (a) Histology of mammary tissue in WT and $LRF^{-/-}$ virgin females and dams that were 24 h into their first lactational period (24 hpp). Data are representative of $n = 2$ (virgin) and $n = 3$ (24 h pp) mice. Scale bar, 50 μm. Corticosterone (b), oxytocin (c), and serum PRL (d) levels were measured in mid- (12 dpc) and late (18 dpc) parturition and within the first 12 h of birth (12 hpp) in $LRF^{-/-}$ females ($n = 10$; KO) and WT females ($n = 16$). All data were plotted with SEM. *, $P = 0.005$, between genotypes in a two-way repeated measures ANOVA across time points; **, $P = 0.002$; ***, $P = 0.001$, in a pairwise multiple comparison procedure (Tukey test).

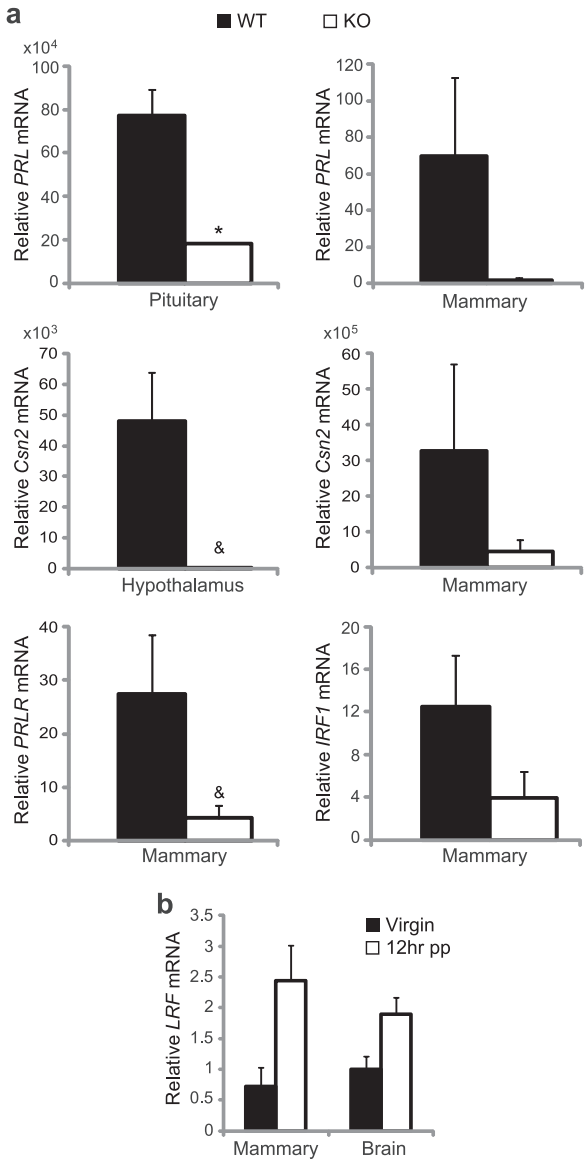

FIG 4 Defective PRL signaling in $LRF^{-/-}$ mice. (a) Relative mRNA levels of genes in the PRL signaling pathway (*PRL*, *Csn2*, *PRLR*, and *IRF-1*) from pituitary, hypothalamus, and mammary epithelium of WT and $LRF^{-/-}$ dams at <12 hpp were measured by qRT-PCR. (b) *LRF* mRNA levels in the brain and mammary epithelium from WT dams at <12 hpp and virgin females, as measured by qRT-PCR. Data were normalized to β-actin and are presented as the averages of three technical repeats of two independent sample sets. All data were plotted with SEM. *, $P = 0.041$; &, P is between 0.050 and 0.100. Multiplication factors are shown above the y axis, where applicable.

mothers that will spontaneously foster pups (46). To investigate if pup death was caused by developmental defects of the pups or poor nurturing by the dam, $LRF^{+/-}$ pups born to $LRF^{-/-}$ mothers and WT fathers were cross-fostered to nursing WT dams within 18 h of birth. Pups were monitored for the presence of milk spots and nest position every 6 h for 3 days. In contrast to non-cross-fostered litters, 77% of cross-fostered pups survived into adulthood (Fig. 2b). These data suggest that maternal factors, not the fitness of the pups, are the cause of poor litter survival.

Nulliparous $LRF^{-/-}$ females show an increase in non-pup-related activities during the pup retrieval test. In many cases, pups were found outside the nest after parturition, suggesting that $LRF^{-/-}$ dams may lack the instinct to nurture pups. We therefore sought to characterize the maternal behavior of $LRF^{-/-}$ female mice using a pup retrieval assay (32, 39). Nulliparous females not previously exposed to juvenile mice were exposed to three healthy, WT pups over a period of 3 days. On the third day, the number of pups retrieved, latency of pup retrieval, and nest quality (data not shown) were similar between genotypes. Once a pup was brought into the nest, however, the time spent in the nest crouching over the pups was significantly reduced in $LRF^{-/-}$ females (Fig. 2c) ($P = 0.0006$). $LRF^{-/-}$ females spent significantly more time engaged in active behaviors such as nest building, digging, and exploring. It thus appears that $LRF^{-/-}$ mice are impaired in specific pup-directed maternal behaviors.

$LRF^{-/-}$ females have decreased pre- and postpartum serum prolactin levels. Pup nursing/suckling is critical for stimulation of lactation as well as of maternal behaviors. After confirming the existence of milk in $LRF^{-/-}$ dams by palpating the mammary tissue around the nipple, we conducted further histological examination of mammary tissues of virgin and primiparous lactating mice. Mammary glands from nonlactating WT and $LRF^{-/-}$ females demonstrated similar rudimentary development of the mammary gland ductal tree with no distinct morphological differences (Fig. 3a, top panels). $LRF^{-/-}$ primiparous lactating dams, however, had marked decreases in the density of terminally differentiated glandular profiles compared to the WT mice (Fig. 3a, bottom panels).

Next, we examined hormone responses related to lactation and maternal responsiveness. Circulating levels of corticosterone, oxytocin, and PRL were measured by ELISA in WT and $LRF^{-/-}$ females during parturition. Blood sera were collected from preg-

nant mice at 12 and 18 days postcoitum (dpc) and within 12 h postpartum (hpp). Plasma corticosterone and oxytocin levels were not significantly different over time between $LRF^{-/-}$ and WT females (Fig. 3b and c) ($P = 0.5930$ and $P = 0.6040$, respectively). Serum PRL levels in pregnant WT females followed a normal pattern in late gestation, increasing significantly from 12 dpc to 18 dpc (Fig. 3d) ($P = 0.001$), which is within the expected range (above 25 ng/ml) to induce lactation (41), followed by a decrease at 12 hpp (Fig. 3d). Conversely, this pattern of circulating PRL concentration was not seen in $LRF^{-/-}$ mice ($P = 0.005$ compared to WT) (Fig. 3d).

PRL signaling pathway is affected in $LRF^{-/-}$ dams. Although serum PRL levels were significantly lower in expecting $LRF^{-/-}$ females, appreciable amounts were still detected (Fig. 3d). This was confirmed by quantitative reverse transcriptase PCR (qRT-PCR), in which *PRL* mRNA levels detected in the pituitary tissues of $LRF^{-/-}$ dams were significantly lower (>5-fold; $P = 0.041$) than those of WT dams, consistent with levels in mammary tissues (Fig. 4a).

To determine if PRL downstream signaling is affected, mRNAs of direct downstream targets were measured by qRT-PCR (Fig. 4a). In the hypothalamus and mammary tissue of lactating $LRF^{-/-}$ females, mRNA levels of *CSN2*, the gene for the major milk protein β-casein, were >15-fold lower than those in WT mice, and PRL receptor (*PRLR*) mRNA levels were reduced 9-fold in mammary tissue of $LRF^{-/-}$ females. Transcription levels of another PRL downstream gene, interferon regulatory factor-1 (*IRF-1*), were 6-fold lower in mammary tissue of $LRF^{-/-}$ dams than in WT mice. In agreement with these data, *LRF* transcripts in WT primiparous dams were 3- and 2-fold more abundant in mammary and brain tissues, respectively, at 12 hpp than in virgin females (Fig. 4b). We noticed that the reduction of PRL downstream gene expression was more pronounced than the levels of PRL itself (Fig. 3d). This should not be surprising as the expression of downstream genes is not solely determined by the level of PRL. Many other factors, such as PRL receptor and its binding proteins (its regulators), other transcription factors, and cofactors, all play important roles in this signaling.

These results suggest that LRF may be a key regulator of the PRL signaling pathway and that PRL misregulation may be the underlying factor for the maternal behavioral defect in $LRF^{-/-}$ mice.

$LRF^{-/-}$ female mice display evidence of hyperactivity and impaired social recognition. To further analyze behaviors of the mutant mice, we continued neurological investigation with a dark-light anxiety test. Although WT and $LRF^{-/-}$ female mice both demonstrated a normal preference for darkness, $LRF^{-/-}$ females spent less time in the dark than WT mice (Fig. 5a, top left) ($P = 0.0136$). A decrease in horizontal activity was noted for both genotypes on the second test day (Fig. 5a, bottom left) (WT, $P = 0.0003$; $LRF^{-/-}$, $P = 0.0014$), suggesting normal habituation to the testing environment; however, $LRF^{-/-}$ females displayed increased horizontal (Fig. 5a, bottom left) ($P = 0.0183$) and vertical locomotor activity (Fig. 5a, bottom right) ($P = 0.0119$).

In a social recognition test, time spent exploring a social stimulus decreased over the training period (tests 1 to 4) for both $LRF^{-/-}$ and WT females (Fig. 5b, left), showing normal habituation. Additionally, time spent exploring each of the familiar stimuli during the training period remained equal at approximately 50%. However, when a novel mouse was introduced in test 5,

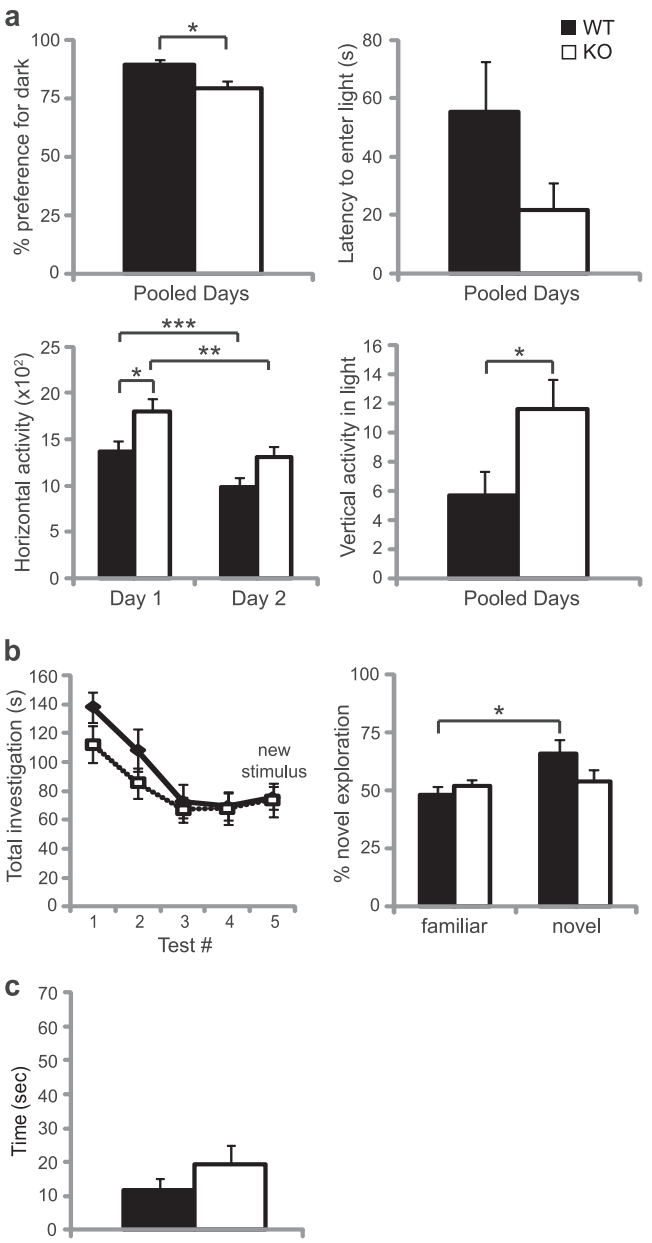

FIG 5 Behavioral assessment of $LRF^{-/-}$ and WT mice. (a) The dark-light anxiety test for female mice. WT ($n = 13$) and $LRF^{-/-}$ ($n = 11$) mice were tested for percent preference for dark, percent latency to enter light, total horizontal activity, and vertical activity in the light half of the chamber. *, $0.01 < P < 0.02$; **, $P = 0.0014$; ***, $P = 0.0003$. (b) Social recognition test for female mice. Total time spent investigating the stimulus mice and proportion of time spent investigating the novel mouse were measured (WT, $n = 6$; $LRF^{-/-}$, $n = 9$). *, $P = 0.0049$. (c) Hidden-reward test for olfaction. WT ($n = 12$) and $LRF^{-/-}$ KO female ($n = 10$) mice were used. All data were plotted with SEM.

although the total amount of time spent exploring both stimuli did not increase (Fig. 5b, left, compare test 4 to 5), WT females spent significantly more time exploring the novel stimulus (Fig. 5b, right) ($P = 0.0049$) while $LRF^{-/-}$ females did not display this preference. Other quantifiable behaviors (such as locomotor activity and self-grooming) were not significantly different between WT and $LRF^{-/-}$ mice (data not shown).

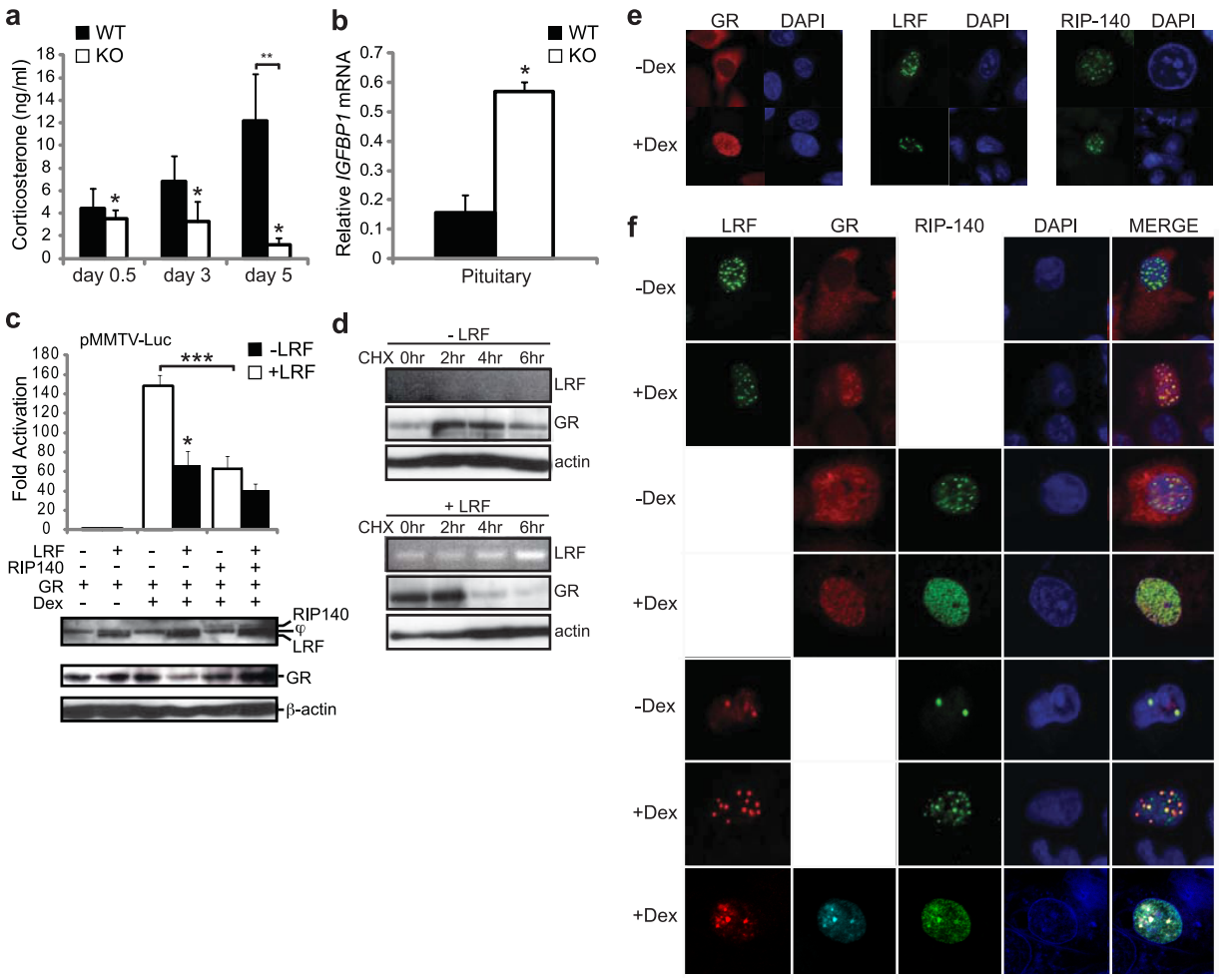

FIG 6 LRF is a negative regulator of the glucocorticoid receptor. (a) Defect in corticosterone secretion in postpartum LRF$^{-/-}$ dams. Corticosterone levels were measured by ELISA from blood serum of LRF$^{-/-}$ females ($n = 5$) and WT females ($n = 5$) at 0.5, 3, and 5 days pp. *, $P = 0.010$ between genotypes by two-way repeated-measures ANOVA across time points. **, $P = 0.010$ in a pairwise multiple comparisons procedure (Holm-Sidak). (b) Misregulation of a downstream gene target of GR, IGFBP1, in mouse pituitary. Relative IGFBP1 mRNA levels were measured by qRT-PCR on total RNA of pituitary from WT and LRF$^{-/-}$ (KO) female mice at <12 hpp. Values are normalized to β-actin. *, $P = 0.010$ in a two-tailed t test. (c) LRF represses GR transactivation as measured by dual-luciferase reporter assays. Western blotting was performed on the same lysates. "j" indicates a nonspecific background band. *, $P = 0.010$; ***, $P = 0.006$ in a two-tailed t test. (d) LRF promotes GR protein degradation. HeLa cells transfected with pSG5-hGR alone (top panel) or cotransfected with pSG5-hGR and pEGFP-LRF (bottom panel) were subjected to CHX treatment for 0, 2, 4, or 6 h in the presence of Dex. Cells were harvested, and Western blotting or RT-PCR was performed on protein extracts. β-Actin was used as a loading control. (e and f) GR colocalizes with LRF in nuclear foci. Confocal microscopic analysis of LRF, GR, and RIP140 subcellular localization in HeLa cells. GFP-LRF and GFP-RIP140 are shown in green; FLAG-LRF and GR are in red except for the triple staining, where GR is shown in cyan. Nuclei were stained with DAPI (blue). Cells were individually transfected (e) or cotransfected (f) for each treatment. All data were plotted with SEM.

To examine the possibility that the impaired social recognition was due to olfactory malfunction, a hidden-reward olfaction test was also performed. No olfactory abnormality was observed in *LRF*$^{-/-}$ female mice (Fig. 5c).

LRF may regulate prolactin signaling through GR. The low serum PRL levels and increased locomotor activity observed in *LRF*$^{-/-}$ females prompted us to investigate possible malfunctions of the HPA axis and glucocorticoid stress responses in these female *LRF*$^{-/-}$ mice. Higher GR activity will result in lower corticosterone levels (15, 19). While corticosterone progressively increased in WT dams over the 5 days, this increase was not observed in *LRF*$^{-/-}$ dams (Fig. 6a) ($P = 0.010$). In fact, at day 3 postpartum, levels were 50% lower in *LRF*$^{-/-}$ dams than in WT mice, and by 5 days postpartum there was a 12-fold reduction (Fig. 6a) ($P =$ 0.010). This suppression of circulating corticosterone in *LRF*$^{-/-}$ dams suggests higher levels of active GR during the postpartum period.

Glucocorticoids are known to be involved in PRL signaling (20, 36) by a mechanism that is largely dependent on the amount of active GR available (21). Insulin growth factor binding protein 1 (IGFBP1) is a downstream target of GR that contains a typical glucocorticoid response element (GRE) in the promoter (26). IGFBP1 is most abundantly synthesized in the liver but has also been detected in other areas of the body and thus is an ideal marker for determining GR activity *in vivo*. We examined *IGFBP1* mRNA levels in various tissues by qRT-PCR in WT and *LRF*$^{-/-}$ dams at <12 hpp. In the hypothalamus and mammary tissue, *IGFBP1* mRNA levels were virtually undetectable, as expected

(data not shown); however, in the pituitary, *IGFBP1* mRNA levels were approximately 4-fold higher in $LRF^{-/-}$ than in WT mice (Fig. 6b) ($P = 0.01$).

To confirm a possible repressive role for LRF in the regulation of GR, we analyzed the effect of LRF on the transcription activation function of GR by reporter assays (Fig. 6c). In the presence of the GR ligand, dexamethasone (Dex), GR activation of the pMMTV-luc reporter, which contains four positive GREs, was increased 150-fold compared to levels in the absence of Dex. Addition of LRF inhibited GR activation of the MMTV promoter by more than 50% ($P = 0.0106$), similar to the effect of receptor-interacting protein RIP140/NRIP1 (nuclear receptor-interacting protein 1) ($P = 0.006$) (59, 63), a known negative regulator of GR (57). When LRF was coexpressed with RIP140 in Dex-treated cells, LRF further repressed GR activity by an additional 23% compared to activity with RIP140 alone.

We noticed that in Dex-treated cells, GR protein levels were reproducibly lower when cotransfected with LRF (Fig. 6c, fourth lane from the left in the Western blot). To determine if LRF promotes GR protein degradation, we conducted a cycloheximide (CHX) assay to examine the protein stability of GR. Since LRF has a half-life of less than 20 min (1), LRF cannot be detected by Western blotting when *de novo* protein synthesis is stopped by CHX treatment. RT-PCR was therefore performed to verify the success of LRF transfection (Fig. 6d). GR concentration increased after 2 h of CHX treatment in the absence of LRF (Fig. 6d, −LRF). Conversely, the GR concentration dropped sharply in LRF-transfected cells (Fig. 6d, +LRF) at 4 h post-CHX treatment and was substantially diminished by 6 h, suggesting a role for LRF in protein degradation of GR.

GR transcriptional activation activity is repressed by receptor-interacting protein RIP140, which recruits GR to nuclear foci (59, 63). Since LRF is known to recruit CREB3 to similar nuclear foci and repress CREB3 transcriptional activity (1), we investigated the intracellular distribution of LRF and GR by confocal microscopy. In the absence of Dex, GR was distributed mainly in the cytoplasm (Fig. 6e). Upon ligand binding (with Dex), GR distribution was diffuse in the nucleus (Fig. 6e). LRF localized to nuclear foci, as previously reported (1), both in the presence and absence of Dex (Fig. 6e). When GR and LRF were cotransfected in untreated cells, results similar to individually transfected cells were observed. When cells were treated with Dex, however, GR was redistributed to the nucleus and colocalized with LRF in foci (Fig. 6f).

Similar to RIP140, LRF has been shown to sequester proteins to nuclear foci and inhibit downstream activation (1). To determine if LRF and RIP140 colocalize and act in a similar fashion to repress GR activity, we studied subcellular localization in cells transfected with either GFP-RIP140 alone or GFP-RIP140 and FLAG-LRF (Fig. 6f). In untreated cells, RIP140 localized to nuclear foci; when cells were treated with Dex, however, the cellular localization of RIP140 was redistributed from nuclear foci into a more diffuse pattern (Fig. 6f), as previously reported (59). Interestingly, in the presence of LRF, RIP140 colocalized with LRF in distinct nuclear foci (Fig. 6f). Additionally, when cells were transfected with FLAG-LRF, GR, and GFP-RIP140 together, all three proteins colocalized in large nuclear foci in the presence of Dex (Fig. 6f). Although the observation that not all available GR or GFP-RIP140 colocalized with LRF in foci might be due to uneven expression levels of these transfected proteins, it may be equally plausible to interpret this observation as evidence supporting our hypothesis

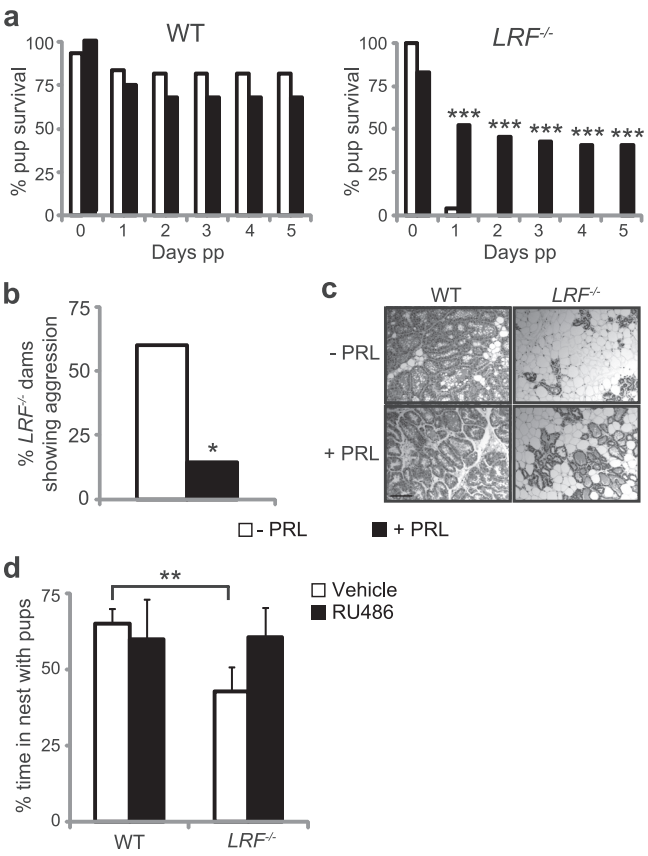

FIG 7 Restoration of maternal neglect in $LRF^{-/-}$ female mice. (a and b) Maternal behavior is improved in $LRF^{-/-}$ dams with exogenous PRL treatment. Pup survival (a) and aggressive behavior toward pups (b) are represented for control (white bars) and PRL-treated (black bars) dams (WT, $n = 6$ control, $n = 7$ treated; $LRF^{-/-}$, $n = 5$ control, $n = 7$ treated). pp, postpartum. (c) Histology of mammary tissue in lactating WT and $LRF^{-/-}$ dams with and without PRL treatment. Scale bar, 50 μm. (d) Spontaneous maternal behavior during the pup retrieval assay is restored in $LRF^{-/-}$ mice with RU486, a GR antagonist. Adult virgin WT and $LRF^{-/-}$ female mice treated with RU486 or vehicle alone were subject to the pup retrieval assay (WT, $n = 4$ vehicle, $n = 5$ treated; $LRF^{-/-}$, $n = 6$ vehicle, $n = 6$ treated). The percentage of time spent in nest with the pups after the first pup was retrieved is shown. All data were plotted with SEM. *, $P = 0.0488$; ***, $P < 0.001$ for PRL treated compared to untreated in a Z-test for proportions. **, $P = 0.027$ in a two-tailed t test.

that LRF as a repressor of GR only attenuates GR signaling during late pregnancy and postpartum and does not shut it off. Not surprisingly, where LRF was absent, GR and GFP-RIP140 were still found to colocalize. These data suggest that LRF may work in concert with RIP140 and repress the transcriptional activity of GR in the same nuclear foci, in which acceleration of GR protein turnover may also be a contributing factor.

PRL supplementation or GR repression by RU486 restores maternal behavior in $LRF^{-/-}$ dams. To determine if low PRL levels were the main cause of the observed maternal behavioral defect, $LRF^{-/-}$ and WT dams were treated with exogenous PRL prior to parturition. As expected, no obvious difference in pup survival rates was observed between untreated and PRL-treated WT dams (Fig. 7a, left). Consistent with our initial data (Fig. 2), most pups born to untreated $LRF^{-/-}$ dams failed to survive past 24 h (Fig. 7a, right), with pups showing evidence of infanticide (such as bite marks and missing limbs) (Fig. 7b). Upon PRL treatment, $LRF^{-/-}$ dams nur-

tured approximately 50% of their litter (Fig. 7a), and aggressive behavior was significantly reduced (Fig. 7b). Histological analysis of mammary tissues showed increased density of terminally differentiated glandular profiles in PRL-treated $LRF^{-/-}$ dams compared to that of untreated mutants (Fig. 7c).

We next sought to assess the importance of LRF repression of GR activity for the maternal behavior deficit and hyperactive nature of $LRF^{-/-}$ mice by exploiting RU486, a GR antagonist. Unfortunately, assays could not be performed on primiparous dams as RU486 causes spontaneous abortion in rodents (56). Instead, virgin female mice were exposed to the pup retrieval assay. As shown previously (Fig. 2), the number of pups retrieved, pup retrieval time, and nest quality were similar for control and RU486-treated mice, regardless of genotype (data not shown). Control-treated $LRF^{-/-}$ mice, however, spent significantly less time in the nest with the pups than WT mice (Fig. 7d, white bars) ($P = 0.034$). Interestingly, RU486-treated $LRF^{-/-}$ mice displayed dramatic improvement in maternal behavior in the time spent in the nest with pups, which was restored to WT levels (Fig. 7d, black bars). This observed restoration of maternal behavior through PRL and RU486 treatment in $LRF^{-/-}$ mice strongly supports the idea that LRF is a repressor of GR, affecting key cell signaling during parturition.

DISCUSSION

In this study, we report the establishment and characterization of a gene knockout mouse line of the recently identified gene, *LRF* (1). We found that LRF is essential for development of maternal behavior as 80% of litters born to $LRF^{-/-}$ females did not survive due to maternal neglect and/or aggression. Although nulliparous $LRF^{-/-}$ females showed the maternal instinct of retrieving pups to the nest, they spent little time tending to the pups. Instead, they showed an increase in non-pup-related active behaviors outside the nest, such as digging and nest building. Since stimulus pups used in the test were born to WT dams and were healthy, the lack of interest shown toward the pups by $LRF^{-/-}$ females cannot be attributed to lack of pup fitness and subsequent inability of pups to provide pup-induced maternal cues.

Insufficient PRL levels and consequent reduced PRL signaling may be the main causes of the maternal behavioral deficit in the $LRF^{-/-}$ mice (Fig. 3 and 4). PRL is a known key hormone in stimulating a rapid maternal response (6, 39). Maternal behavior is delayed in rats treated with bromocriptine, which blocks PRL secretion (7, 39). Disruption of the *PRLR* gene causes impairment of maternal behaviors, clearly indicating a requirement for PRL signaling (39). Although nulliparous $PRL^{-/-}$ females, like WT mice, retrieved and crouched over foster pups, within 30 min after placement of the pups (29), no other behavioral assessment was reported. The fact that $PRL^{-/-}$ mice are completely infertile makes it impossible to examine these mice for pup-induced maternal responses at parturition. It is possible that other lactogenic hormones that are known to activate the PRLR, such as placental lactogen, which is synthesized during gestation (4), contributed to the maternal instinct observed in the pup retrieval assays of $PRL^{-/-}$ and $LRF^{-/-}$ virgin mice (Fig. 2c).

The low level of PRL in $LRF^{-/-}$ mice (Fig. 3d) may be due to misregulation of GR activity in the absence of repression by LRF, especially during parturition. A factor central to PRL levels is the activity of GR during parturition. PRL synthesis is primarily regulated by Pit-1 (17, 23, 40, 50); GR represses PRL synthesis (3, 11, 53), possibly through interference with the Pit-1 binding ability to the PRL promoter (47). WT mice were found to have elevated levels of LRF in the brain (Fig. 4), which has a repressive effect on GR (Fig. 6c). Without such inhibition in $LRF^{-/-}$ mice, higher GR activities may result in reduced levels of PRL. The widespread distribution of *LRF* expression in WT mouse brain (see Fig. S1 in the supplemental material), the elevated level of *IGFBP1*, and lower levels of postpartum corticosterone (Fig. 6a and b) in $LRF^{-/-}$ mice support the observation that LRF negatively regulates GR activity in mice. Complete restoration of maternal behavior in the pup retrieval assay after RU486 treatment (Fig. 7a and b) further substantiates this notion. In cell culture, LRF protein colocalizes with the known GR repressor RIP140 and inhibits transcriptional function of GR (Fig. 6c). Since LRF has a short half-life (estimated at <20 min) and promotes CREB3 degradation (1), the observed acceleration of GR protein turnover by LRF (Fig. 6d) may also occur *in vivo*, which could be due to direct interaction between GR and LRF or indirect interaction through RIP140 recruitment of GR to the discrete LRF/RIP140 nuclear foci.

Although low PRL levels may be a key causative factor, the severity of the maternal defect is likely due to the compound effect of misregulated HPA axis and abnormal GR stress signaling in the $LRF^{-/-}$ mice (Fig. 8). The severity of pup loss from $LRF^{-/-}$ dams and only partial phenotype rescue by PRL treatment may imply that low levels of PRL are not the sole cause of the maternal behavior phenotype. It is known that proper function of the HPA axis is crucial for the onset of parturition and lactation in late

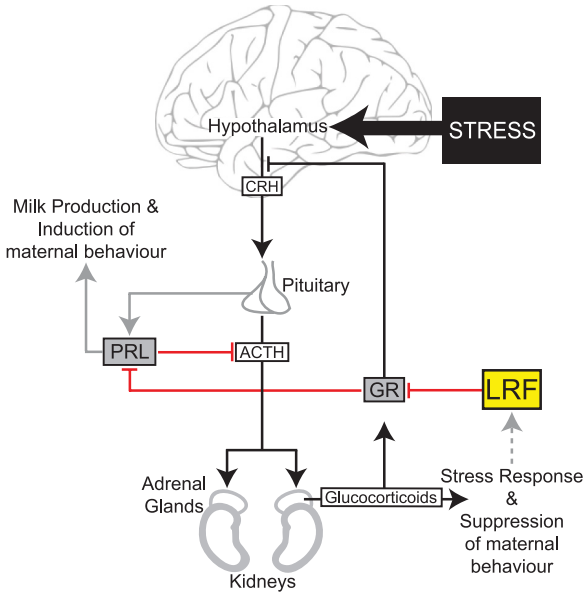

FIG 8 Working model for the cellular function of LRF in GR regulation of the HPA axis and PRL signaling. Upon stress (e.g., at parturition), *LRF* gene activation is paralleled with upregulation of the HPA axis (black arrows), resulting in secretion of high levels of glucocorticoids via induction of hormones from the hypothalamus and pituitary. High glucocorticoid levels activate GR, which results in downstream activation of target genes and negative feedback inhibition of the stress response. LRF represses GR activity (shown in red) likely through recruitment to discrete nuclear foci. Within the pituitary, repression of high levels of GR by LRF leads to PRL synthesis and secretion, triggering the PRL-induced maternal response (gray arrows). In other regions of the brain, repression of high GR levels results in the tight regulation of HPA-related processes. ACTH, adrenocorticotrophic hormone; CRH, corticotrophin-releasing hormone.

pregnancy (18), as well as for milk production and maternal care stimulation (49). During the postpartum period, HPA responses to stress are attenuated (10, 55) to benefit the mother by relieving stress and by preventing stress-induced inhibition of lactation and immune function (8, 16, 60). Currently, factors that regulate postpartum HPA axis activity are unclear (2, 44). HPA axis dysfunction, however, has long been associated with major mood disorders and postpartum depression (9, 16).

GR plays a critical role in termination of stress responses through negative feedback inhibition of the HPA axis (15, 19). Thus, improper regulation of GR in $LRF^{-/-}$ mice, as suggested here, may directly interfere with induction of the maternal response and contribute to postpartum depression-like behavior. This notion seems further supported by a report in which serum PRL levels were abnormally low in breast-feeding mothers that were classified as clinically depressed (27, 28).

Hyperactivity of $LRF^{-/-}$ females in the dark-light test and during the pup retrieval assay also corroborates a possible role for LRF in regulation of the HPA axis. Without the control of GR by LRF, GR-mediated feedback inhibition of HPA axis stimulation by stress may be missing, leading to hyperactivity. Since chronic stimulation of the HPA axis is known to impair social recognition performance (58), the observed impairment of $LRF^{-/-}$ female mice, as shown by the social recognition test, implies prolonged HPA axis activity, possibly due to the misregulation of GR. It should be noted that although the hyperactivity observed in $PRL^{-/-}$ mice may contribute to the maternal behavioral deficiency, it is unlikely the cause of the defect as hyperactivity is not necessarily linked to poor maternal responses (42).

It is known that prolonged postpartum treatment with high doses of corticosterone results in reduced maternal behavior and hippocampal cell proliferation, leading to depression-like behavior in the dam (8). Although corticosterone levels were not significantly different between $LRF^{-/-}$ and WT females during pregnancy (Fig. 3b), without the repression of GR by LRF in the $LRF^{-/-}$ mice, glucocorticoid signaling would be affected (Fig. 6a). Consistent with this hypothesis, $LRF^{-/-}$ mice displayed a phenotype similar to that of mice treated with high levels of corticosterone, including hyperactivity and a deficit in maternal instinct, behaviors which are often associated with depression (61). We thus postulate that, through modulating the activity of GR or sensitivity to glucocorticoids, LRF plays an important role in PRL signaling, misregulation of which leads to a defect in maternal behavior in $LRF^{-/-}$ mice (Fig. 8). However, more research is required to understand the effects of stress hormones during reproduction and their effects on the brain and behavior of mother and offspring.

It was noted that $LRF^{-/-}$ female mice spent more time in the light than the WT mice in the dark-light anxiety test (Fig. 5a) although elevated anxiety-like behavior is typically believed to be linked to elevated GR activity. In fact, the overall findings based on GR transgenic/knockout mouse models are inconsistent. For instance, neither forebrain GR overexpressors, the GRov mice (62), nor whole-mouse GR overexpressors, the YGR mice (51), show differences in the open-field anxiety test. While GRov mice display increased anxiety-related measures in the elevated plus-maze test, YGR mice do not show any differences in the elevated zero-maze test (reviewed in references 14 and 35).

The observed maternal behavioral defect in $LRF^{-/-}$ mice has characteristics of postpartum depression in humans, which affects 15% of new mothers (25). There is also a clear link between elevated glucocorticoid signaling, a misregulated HPA axis, and depression (33, 43, 54). The underlying mechanism, however, is unclear. Here, we provide strong evidence suggesting that LRF, via negative regulation of GR, plays a key role in HPA axis attenuation and prolactin signaling as well as in maternal behavior (Fig. 8). These mice may thus provide a valuable animal model for studying the responses of the HPA axis to stress and the related human behaviors.

ACKNOWLEDGMENTS

This work was supported by the Canadian Institutes for Health Research (MOP53186) and Natural Sciences and Engineering Research Council of Canada (238950-06).

We thank the Central Animal Facility at the University of Guelph. We thank Andrew Bendall, Timothy Audas, Yaping Jin, Cheryl Cragg, Graham Smith, Amy Clipperton Allen, Anna Phan, Jennifer Brisbin, Melanie Wills, Adam McCluggage, and Alyssa Lima, who helped with data collection, provided technical assistance, and/or contributed conceptually to the project. We thank Johanna Zilliacus for pEGFP-RIP140, Ronald Evans for pMMTV-Luc, and Jorma Palvimo for pSG5-hGR plasmids.

REFERENCES

1. **Audas TE, Li Y, Liang G, Lu R.** 2008. A novel protein, Luman/CREB3 recruitment factor, inhibits Luman activation of the unfolded protein response. Mol. Cell. Biol. **28**:3952–3966.
2. **Bachelot A, Binart N.** 2007. Reproductive role of prolactin. Reproduction **133**:361–369.
3. **Berwaer M, et al.** 1991. Multihormonal regulation of the human prolactin gene expression from 5000 bp of its upstream sequence. Mol. Cell Endocrinol. **80**:53–64.
4. **Bole-Feysot C, Goffin V, Edery M, Binart N, Kelly PA.** 1998. Prolactin (PRL) and its receptor: actions, signal transduction pathways and phenotypes observed in PRL receptor knockout mice. Endocr. Rev. **19**:225–268.
5. **Bridges RS, Mann PE.** 1994. Prolactin-brain interactions in the induction of material behavior in rats. Psychoneuroendocrinology **19**:611–622.
6. **Bridges RS, Numan M, Ronsheim PM, Mann PE, Lupini CE.** 1990. Central prolactin infusions stimulate maternal behavior in steroid-treated, nulliparous female rats. Proc. Natl. Acad. Sci. U. S. A. **87**:8003–8007.
7. **Bridges RS, Ronsheim PM.** 1990. Prolactin (PRL) regulation of maternal behavior in rats: bromocriptine treatment delays and PRL promotes the rapid onset of behavior. Endocrinology **126**:837–848.
8. **Brummelte S, Galea LA.** 2010. Chronic corticosterone during pregnancy and postpartum affects maternal care, cell proliferation and depressive-like behavior in the dam. Horm. Behav. **58**:769–779.
9. **Brunton PJ, Russell JA.** 2008. The expectant brain: adapting for motherhood. Nat. Rev. Neurosci. **9**:11–25.
10. **Brunton PJ, Russell JA, Douglas AJ.** 2008. Adaptive responses of the maternal hypothalamic-pituitary-adrenal axis during pregnancy and lactation. J. Neuroendocrinol. **20**:764–776.
11. **Camper SA, Yao YA, Rottman FM.** 1985. Hormonal regulation of the bovine prolactin promoter in rat pituitary tumor cells. J. Biol. Chem. **260**:12246–12251.
12. **Choleris E, et al.** 2003. An estrogen-dependent four-gene micronet regulating social recognition: a study with oxytocin and estrogen receptor-alpha and -beta knockout mice. Proc. Natl. Acad. Sci. U. S. A. **100**:6192–6197.
13. **Choleris E, et al.** 2006. Involvement of estrogen receptor alpha, beta and oxytocin in social discrimination: a detailed behavioral analysis with knockout female mice. Genes Brain Behav. **5**:528–539.
14. **Chourbaji S, Gass P.** 2008. Glucocorticoid receptor transgenic mice as models for depression. Brain Res. Rev. **57**:554–560.
15. **Claes S.** 2009. Glucocorticoid receptor polymorphisms in major depression. Ann. N. Y. Acad. Sci. **1179**:216–228.
16. **Cowen PJ.** 2010. Not fade away: the HPA axis and depression. Psychol. Med. **40**:1–4.
17. **Crenshaw EB, Kalla K, Simmons DM, Swanson LW, Rosenfeld MG.** 1989. Cell-specific expression of the prolactin gene in transgenic mice is controlled by synergistic interactions between promoter and enhancer elements. Genes Dev. **3**:959–972.

17a. **Dai K-S, Liew C-C.** 2001. A novel human striated muscle RING zinc finger protein, SMRZ, interacts with SMT3b via its RING domain. J. Biol. Chem. **276**:23992–23999.
18. **de Greef WJ, van der Schoot P.** 1983. Effect of adrenalectomy on the regulation of ovarian function during lactation in the rat. J. Endocrinol. **98**:233–240.
19. **de Kloet ER, Vreugdenhil E, Oitzl MS, Joels M.** 1998. Brain corticosteroid receptor balance in health and disease. Endocr. Rev. **19**:269–301.
20. **Doppler W, Hock W, Hofer P, Groner B, Ball RK.** 1990. Prolactin and glucocorticoid hormones control transcription of the β-casein gene by kinetically distinct mechanisms. Mol. Endocrinol. **4**:912–919.
21. **Doppler W, et al.** 2001. Expression level-dependent contribution of glucocorticoid receptor domains for functional interaction with STAT5. Mol. Cell. Biol. **21**:3266–3279.
22. **Doucas V, Tini M, Egan DA, Evans RM.** 1999. Modulation of CREB binding protein function by the promyelocytic (PML) oncoprotein suggests a role for nuclear bodies in hormone signaling. Proc. Natl. Acad. Sci. U. S. A. **96**:2627–2632.
23. **Fox SR, et al.** 1990. The homeodomain protein, Pit-1/GHF-1, is capable of binding to and activating cell-specific elements of both the growth hormone and prolactin gene promoters. Mol. Endocrinol. **4**:1069–1080.
24. **Good TC, Harris KK, Ihunnah CA.** 2005. Corticosteroids as potential mechanism regulating variability in reproductive success in monogamous oldfield mice (Peromyscus polionotus). Physiol. Behav. **86**:96–102.
25. **Goodman SH.** 2007. Depression in mothers. Annu. Rev. Clin. Psychol. **3**:107–135.
26. **Goswami R, Lacson R, Yang E, Sam R, Unterman T.** 1994. Functional analysis of glucocorticoid and insulin response sequences in the rat insulin-like growth factor-binding protein-1 promoter. Endocrinology **134**: 736–743.
27. **Harris B, et al.** 1989. The hormonal environment of post-natal depression. Br. J. Psychiatry **154**:660–667.
28. **Hendrick V, Altshuler LL, Suri R.** 1998. Hormonal changes in the postpartum and implications for postpartum depression. Psychosomatics **39**: 93–101.
29. **Horseman ND, et al.** 1997. Defective mammopoiesis, but normal hematopoiesis, in mice with a targeted disruption of the prolactin gene. EMBO J. **16**:6926–6935.
30. **Horton BM, Holberton RL.** 2009. Corticosterone manipulations alter morph-specific nestling provisioning behavior in male white-throated sparrows, Zonotrichia albicollis. Horm. Behav. **56**:510–518.
31. **Insel TR, Young L, Wang Z.** 1997. Central oxytocin and reproductive behaviours. Rev. Reprod. **2**:28–37.
32. **Jin SH, Blendy JA, Thomas SA.** 2005. Cyclic AMP response element-binding protein is required for normal maternal nurturing behavior. Neuroscience **133**:647–655.
33. **Jolley SN, Elmore S, Barnard KE, Carr DB.** 2007. Dysregulation of the hypothalamic-pituitary-adrenal axis in postpartum depression. Biol. Res. Nurs. **8**:210–222.
34. **Kang H, Kim YS, Ko J.** 2009. A novel isoform of human LZIP negatively regulates the transactivation of the glucocorticoid receptor. Mol. Endocrinol. **23**:1746–1757.
35. **Kolber BJ, Wieczorek L, Muglia LJ.** 2008. Hypothalamic-pituitary-adrenal axis dysregulation and behavioral analysis of mouse mutants with altered glucocorticoid or mineralocorticoid receptor function. Stress **11**: 321–338.
36. **Lechner J, et al.** 1997. Promoter-dependent synergy between glucocorticoid receptor and Stat5 in the activation of beta-casein gene transcription. J. Biol. Chem. **272**:20954–20960.
37. **Lindsay JR, Nieman LK.** 2005. The hypothalamic-pituitary-adrenal axis in pregnancy: challenges in disease detection and treatment. Endocr. Rev. **26**:775–799.
38. **Lu R, Yang P, O'Hare P, Misra V.** 1997. Luman, a new member of the CREB/ATF family, binds to herpes simplex virus VP16-associated host cellular factor. Mol. Cell. Biol. **17**:5117–5126.
39. **Lucas BK, Ormandy CJ, Binart N, Bridges RS, Kelly PA.** 1998. Null mutation of the prolactin receptor gene produces a defect in maternal behavior. Endocrinology **139**:4102–4107.
40. **Mangalam HJ, et al.** 1989. A pituitary POU domain protein, Pit-1, activates both growth hormone and prolactin promoters transcriptionally. Genes Dev. **3**:946–958.
41. **Markoff E, Talamantes F.** 1981. Serum placental lactogen in mice in relation to day of gestation and number of conceptuses. Biol. Reprod. **24**:846–851.
42. **Marsh DJ, et al.** 2002. Melanin-concentrating hormone 1 receptor-deficient mice are lean, hyperactive, and hyperphagic and have altered metabolism. Proc. Natl. Acad. Sci. U. S. A. **99**:3240–3245.
43. **McIsaac SA, Young AH.** 2009. The role of hypothalamic pituitary-adrenal axis dysfunction in the etiology of depressive disorders. Drugs Today (Barc.) **45**:127–133.
44. **Meinlschmidt G, Martin C, Neumann ID, Heinrichs M.** 2010. Maternal cortisol in late pregnancy and hypothalamic-pituitary-adrenal reactivity to psychosocial stress postpartum in women. Stress **13**:163–171.
45. **Moilanen A-M, Karvonen U, Poukka H, Janne OA, Palvimo JJ.** 1998. Activation of androgen receptor function by a novel nuclear protein kinase. Mol. Biol. Cell **9**:2527–2543.
46. **Nagasawa H, Miyamoto M, Fujimoto M.** 1973. Reproductivity in inbred strains of mice and project for their efficient production. Jikken Dobutsu. **22**:119–126. (In Japanese.)
47. **Nalda AM, Martial JA, Muller M.** 1997. The glucocorticoid receptor inhibits the human prolactin gene expression by interference with Pit-1 activity. Mol. Cell Endocrinol. **134**:129–137.
48. **Nord AS, et al.** 2006. The International Gene Trap Consortium website: a portal to all publicly available gene trap cell lines in mouse. Nucleic Acids Res. **34**:D642–D648.
49. **Patin V, et al.** 2002. Effects of prenatal stress on maternal behavior in the rat. Brain Res. Dev. Brain Res. **139**:1–8.
50. **Peers B, et al.** 1990. Regulatory elements controlling pituitary-specific expression of the human prolactin gene. Mol. Cell. Biol. **10**:4690–4700.
51. **Ridder S, et al.** 2005. Mice with genetically altered glucocorticoid receptor expression show altered sensitivity for stress-induced depressive reactions. J. Neurosci. **25**:6243–6250.
52. **Rosenblatt JS.** 1967. Nonhormonal basis of maternal behavior in the rat. Science **156**:1512–1513.
53. **Sakai DD, et al.** 1988. Hormone-mediated repression: a negative glucocorticoid response element from the bovine prolactin gene. Genes Dev. **2**:1144–1154.
54. **Schule C, et al.** 2009. The combined dexamethasone/CRH Test (DEX/CRH test) and prediction of acute treatment response in major depression. PLoS One **4**:e4324. doi:10.1371/journal.pone.0004324.
55. **Slattery DA, Neumann ID.** 2008. No stress please! Mechanisms of stress hyporesponsiveness of the maternal brain. J. Physiol. **586**:377–385.
56. **Spitz IM, Bardin CW.** 1993. Mifepristone (RU 486)—a modulator of progestin and glucocorticoid action. N. Engl. J. Med. **329**:404–412.
57. **Subramaniam N, Treuter E, Okret S.** 1999. Receptor interacting protein RIP140 inhibits both positive and negative gene regulation by glucocorticoids. J. Biol. Chem. **274**:18121–18127.
58. **Tang AC, Reeb BC, Romeo RD, McEwen BS.** 2003. Modification of social memory, hypothalamic-pituitary-adrenal axis, and brain asymmetry by neonatal novelty exposure. J. Neurosci. **23**:8254–8260.
59. **Tazawa H, et al.** 2003. Regulation of subnuclear localization is associated with a mechanism for nuclear receptor corepression by RIP140. Mol. Cell. Biol. **23**:4187–4198.
60. **Tu H, et al.** 2005. Cytokine regulation of tryptophan metabolism in the hypothalamic-pituitary-adrenal (HPA) axis: implications for protective and toxic consequences in neuroendocrine regulation. Cell Mol. Neurobiol. **25**:673–680.
61. **Vollmayr B, Mahlstedt MM, Henn FA.** 2007. Neurogenesis and depression: what animal models tell us about the link. Eur. Arch. Psychiatry Clin. Neurosci. **257**:300–303.
62. **Wei Q, et al.** 2004. Glucocorticoid receptor overexpression in forebrain: a mouse model of increased emotional lability. Proc. Natl. Acad. Sci. U. S. A. **101**:11851–11856.
63. **Zilliacus J, et al.** 2001. Regulation of glucocorticoid receptor activity by 14-3-3-dependent intracellular relocalization of the corepressor RIP140. Mol. Endocrinol. **15**:501–511.